The icosahedral quasiperiodic tiling and its self-similarity

Ruth Maria Katharina Dietl and Jost-Hinrich Eschenburg

To Paul Hildebrandt, Zometool Inc.

Abstract. We investigate a 3-dimensional analogue of the Penrose tiling, a class of 3-dimensional aperiodic tilings whose edge vectors are the vertex vectors of a regular icosahedron. It arises by an equivariant orthogonal projection of the unit lattice in euclidean 6-space with its natural representation of the icosahedral group, given by its action on the 6 icosahedral diagonals (with orientation). The tiling has a canonical subdivision by a similar tiling ("deflation"). We give an essentially local construction of this subdivision, independent of the actual position inside the tiling. In particular we show that the subdivisions of the edges, faces and tiles (with some restriction) are unique.

1. Introduction

In 1974 *Roger Penrose* (see [19]) constructed a class of tilings of the euclidean plane which are not periodic but quasiperiodic, a concept introduced by Harald Bohr [2] in 1924. The tilings consist of two congruence types of tiles which are the two isosceles triangles formed by edges and diagonals of a regular pentagon. The triangular tiles compose pairwise to two types of rhombs all of whose edges are parallel to the vertex vectors of a fixed regular pentagon. These tilings enjoy some kind of self-similarity: the tiles are subdivided uniquely by smaller tiles with equal shapes, and also these can be subdivided again and again, always by the same rule. On every stage, the small tiles together form another Penrose tiling.

This process is called "deflation", its inverse process "inflation". This property of the tiling follows in an elementary way from the pentagon geometry [7], and it is a purely local property: the subdivision in each part is independent from the rest of the tiling. But many (not all, see [9]) of these tilings can be obtained also globally by a 2-dimensional projection of part of the 5-dimensional standard grid $\mathbb{Z}^5 \subset \mathbb{R}^5$. This method has been introduced first by *Nicolaas Govert de Bruijn* [4], see also [1]. It can be extended to other dimensions, see subsection 2.1, and it is a useful tool in order to construct many other tilings in euclidean 2-plane and 3-space. However, most of these tilings do not admit a subdivision for which a local construction is possible, see [8].

The physicist *Alan Mackay* is one of the first observing possible applications of the Penrose tiling in the field of solid state physics, see [15],[16]. With the discovery of quasicrystals by *Dan Shechtman* in 1982 for which he was awarded with the Nobel Prize for chemistry in 2011, the interest in aperiodic tilings started growing: neighbouring disciplines such as crystallography, chemistry or physics considered these tilings as possible models for quasicrystals. In this context also the question of a 3-dimensional generalization of the Penrose tiling of the plane arised. Some years earlier, in 1976, *Robert Ammann*, considering himself as an "amateur doodler with math background" [20, p.11], has already proposed such a generalization: two different types of rhombohedra can tile the space only aperiodically if they are marked in a certain way, see [20],[21]. These rhombohedra have been described earlier by Kowalewski [14] in connection with 6-dimensional geometry; for details see subsection "Coxeter's Golden Isozonohedra" in our Appendix. In 1984 *Peter Kramer* and *Roberto Neri* provided a theoretical approach for such tilings consisting of Kowalewski's rhombohedra, see [13]. For this purpose they worked with the projection from $\mathbb{R}^{12}$ via $\mathbb{R}^6$ to $\mathbb{R}^3$ and introduced a "Hexagrid" in $\mathbb{R}^3$ as an analogue to de Bruijn's "Pentagrid" in $\mathbb{R}^2$. Furthermore they associated these tilings with the icosahedral group, isomorphic to A_5. Since these tilings have all edges parallel to the vertex vectors of a fixed regular icosahedron, they will be called *icosahedral tilings*. *Michel Duneau* and *André Katz* answered some important questions concerning the self-similarity properties of this tiling in 1986, see [10]: the scaling factor is Φ^3 (where Φ denotes the *golden ratio*; in case of the Penrose tiling of the plane the scaling factor is Φ), furthermore they showed that the tiles can't be subdivided in a unique way by deflation. The question how a possible subdivision of the two tiles looks like was not addressed. At the same time also the Japanese *Tohru Ogawa* dealt with the icosahedral tiling, see [17],[18]. He generated the tiling by inflation and distinguished two parts for each tile ("skeleton part" and "internal part"). Some years later, Ogawa also worked with a projection method and presented the different types of vertices for icosahedral tilings.

In this paper the problem of a locally defined subdivision for the icosahedral tiling is investigated, more precisely, for the class of 3-dimensonal tilings of Kramer/Neri and Ogawa where in some sense the pentagon (from the Penrose tiling of the plane) is replaced by the icosahedron. The article is based on the thesis of the first named

author, see [6]. As described above the question of a local construction has some physical significance, however this paper follows a purely mathematical course and it is based on geometry. It shows how to understand the icosahedral tiling just by elementary local geometric constructions. In section 2 starting from the projection method from 6 to 3 dimensions, the two tiles are constructed and the specific deflation is determined. Section 3 investigates what happens to the tiles under deflation: do these tilings generated by the projection method allow a unique locally defined subdivision, like the Penrose tilings? Or at least, are there certain invariant substructures present in the subdivision of every tiling?

The main result of this paper is the construction of such an invariant substructure in each tile, having the full symmetry of the tile. It determines the subdivision completely up to small gaps which allow several fillings; these fillings just differ by symmetries which however do not extend to the ambient tiling. Since the local structure of the tilings can be read off from the subdivisions of tiles, our result shows that the icosahedral tiling is essentially determined locally.

2. Generating Icosahedral tilings

2.1. Projection method

We describe first a general form of the projection method which includes the cases of de Bruijn [4] and Kramer-Neri [13]. The space $\mathbb{R}^d$ on which the tiling will be constructed is considered as a d-dimensional affine subspace $E \subset \mathbb{R}^n$. We call $\mathbb{R}^n$ the *ambient space* and $E \cong \mathbb{R}^d$ the *projection space*. The vertex set $M_E \subset E$ of the tiling is the orthogonal projection onto E of the set of "admissible" integer vectors, those in the "strip" $\Sigma = E + C^n$ where $C = (-\frac{1}{2}, +\frac{1}{2})$ is the centered unit interval,

$$M_E = \pi_E(\mathbb{Z}^n \cap \Sigma). \tag{2.1}$$

The tiles are projections of d-dimensional faces of the $\mathbb{Z}^n$-tiling in $\mathbb{R}^n$; more precisely, a d-dimensional face is projected onto a tile in E if and only if all its vertices are admissible. This gives a tiling when E is in general position with respect to the shifted lattice $(\mathbb{Z} + \frac{1}{2})^n$ which means that any point $x = (x_1, \ldots, x_n) \in E$ has at most d coordinates $x_i \in \mathbb{Z} + \frac{1}{2}$, see e.g. [23].

Additionally, let us assume there is a a group G of orthogonal integer matrices on $\mathbb{R}^n$. Then G preserves the cube $C^n \subset \mathbb{R}^n$. Suppose further that G preserves also the linear subspace E_o parallel to E in the sense that $E = E_o + a$ for some $a \in \mathbb{R}^n$. Let $x_o \in E$ be any point close enough to some integer point $z_o \in \mathbb{Z}^n$. Then G (more precisely, the conjugate group $t_{z_o} G t_{-z_o}$ where $t_{z_o}(x) = x + z_o$ is the translation by z_o) acts on the strip $\Sigma' = E_o + z_o + C^n$ which is close to $\Sigma = E_o + x_o + C^n$, and hence M_E has an almost G-symmetry, a G-symmetry which fails only for those admissible points $z \in \Sigma$ with $z \notin \Sigma'$.

In our case we have $n = 6$ and $d = 3$, and the group G is the group of rotations and reflections of a regular icosahedron (isomorphic to $A_5 \times \mathbb{Z}_2$ where A_5 is the group

of even permutations of $\{1, \ldots, 5\}$). However, we start with $\mathbb{R}^{12}$. Its standard basis $\{c_1, \ldots, c_{12}\}$ will be denoted also as $\{a_1, \ldots, a_6, b_1, \ldots, b_6\}$. We assign these vectors to the 12 vertices $v_1, \ldots, v_{12}$ of the icosahedron in $\mathbb{R}^3$ in the following way: if a_6 is assigned to some vertex v_6, then $a_1, \ldots, a_5$ will be assigned to the five vertices $v_1, \ldots, v_5$ which are the direct neighbours of v_6, in their cyclic ordering. Moreover, we require that b_i and a_i are assigned to antipodal vertices, for $i = 1, \ldots, 6$. Then the antipodal map $-I$ on $\mathbb{R}^3$ is represented by the permutation of the basis

$$A : a_i \mapsto b_i, \quad b_i \mapsto a_i, \text{ for } i = 1, \ldots, 6. \tag{2.2}$$

Let W and W' be the eigenspaces of A corresponding to the eigenvalues -1 and 1, hence

$$\begin{aligned} W &= \operatorname{Span}\{a_i - b_i : i = 1, \ldots, 6\} \\ W' &= \operatorname{Span}\{a_i + b_i : i = 1, \ldots, 6\} \end{aligned}$$

Now the symmetry group G of the icosahedron becomes a group of 12×12-matrices permuting the standard basis like the vertex set of the icosahedron. Clearly G is centralized by A, hence the eigenspaces W and W' are 6-dimensional representation spaces of G. From now on we will restrict our attention only to W.[1] We identify the eigenspace W with $\mathbb{R}^6$ using the basis $e_i := a_i - b_i$ for $1 \le i \le 6$ and G permutes the vectors $\pm e_1, \ldots, \pm e_6$ like the oriented diagonals of the icosahedron. Furthermore we consider the linear map U on $\mathbb{R}^{12}$, commuting with G, which is defined as follows:

$$U : c_i \mapsto \sum \text{ direct neighbours of } c_i \quad \text{for all } 1 \le i \le 12. \tag{2.3}$$

The subspace W is kept invariant by U and is decomposed into the G-invariant eigenspaces of U.

Theorem 2.1. *The eigenvalues of U on W are $\pm\sqrt{5}$. The eigenspaces $W_\pm$ are 3-dimensional G-invariant irrational subspaces.*

Proof. Put $s_i = \frac{1}{\sqrt{5}} U(e_i)$. Then

$$U(e_6) = \sqrt{5}\, s_6 \quad \text{and} \quad U(s_6) = \sqrt{5}\, e_6$$

The first equality is clear by definition, the second one follows from $\sum_{i=1}^5 U(e_i) = 5 e_6$, this is because all neighbours $\ne e_6$ come in antipodal pairs and cancel each other. Thus U keeps the plane $\operatorname{Span}(e_6, s_6)$ invariant and has eigenvalues $\pm\sqrt{5}$ with eigenvectors $e_6 \pm s_6$. A similar statement holds for $\operatorname{Span}(e_i, s_i)$ for $i = 1, \ldots, 5$. The eigenvectors $\pm(e_i + s_i)$ corresponding to the eigenvalue $\sqrt{5}$ form a G-orbit with the geometry of the vertex set of an icosahedron with radius $\sqrt{2}$, thus they span a 3-dimensional subspace $W_+ \subset W$. The same holds for the eigenvectors $\pm(e_i - s_i)$ corresponding to the eigenvalue $-\sqrt{5}$.

---

[1] W' contains the vector $e = \sum_i (a_i + b_i)$ fixed unter A_5, and the orthogonal complement $W'' = W' \ominus \mathbb{R}\, e$ is a 5-dimensional irreducible representation space of A_5. In fact, the map U defined below is a multiple of the identity on W''. There is no G-invariant 3-dimensional subspace in W'.

Next we show that $W_\pm$ is an irrational subspace, i.e. $W_\pm$ does not contain any nonzero integer vector. Suppose we have such a vector $0 \neq v \in W_\pm \cap \mathbb{Z}^6$. Then $gv \in W_\pm \cap \mathbb{Z}^6$ for any $g \in G$. Since $W_\pm$ is irreducible for G, these vectors span $W_\pm$. Thus $W_\pm$ is spanned by integer vectors, and therefore $W_\pm \cap \mathbb{Z}^6$ is a lattice preserved by G. But this contradicts to the crystallographic restriction since G contains rotations of order 5 in 3-space which cannot preserve a lattice. $\qquad\square$

Now we put

$$S := 2I - U \tag{2.4}$$

having eigenvalues $2 \mp \sqrt{5}$ on $W_\pm$. Since $(2 + \sqrt{5})(2 - \sqrt{5}) = -1$, the matrix S on $W = \mathbb{R}^6$ is integer invertible. Observe that $2 + \sqrt{5} = \Phi^3$ where $\Phi = \frac{1}{2}(1 + \sqrt{5})$ is the *golden ratio*, the positive solution of the equation $\Phi^2 = \Phi + 1$, while $2 - \sqrt{5} = -\varphi^3$ where $\varphi = \Phi - 1 = \frac{1}{\Phi}$. The space

$$F := W_- \tag{2.5}$$

will be called *orthogonal space*. Choosing $a \in F$ suitably we can arrange that the affine subspace

$$E = W_+ + a \tag{2.6}$$

avoids any point $x \in \mathbb{R}^6$ with more than three coordinates in $\mathbb{Z} + \frac{1}{2}$ (general position).[2] By projecting all integer points inside the 6-dimensional strip $\Sigma = E + C^6$ orthogonally onto E we obtain the corresponding *icosahedral tiling*[3] $M_E = \pi_E(\Sigma \cap \mathbb{Z}^6)$, cf. (2.1). The basis vectors $e_1, \ldots, e_6$ of the ambient space W project onto E and F to the vectors

$$\pm v_i = \pi_E(\pm e_i), \tag{2.7}$$

$$\pm w_i = \pi_F(\pm e_i), \tag{2.8}$$

$i = 1 \ldots 6$, in the way that both $\pm v_i$ and $\pm w_i$ point to the 12 vertices of an icosahedron, but in two different parametrisations.[4] Therefore the terms *(basic) vector* $\pm v_i$ resp. $\pm w_i$ and *vertex (vector) of the icosahedron* $\pm v_i$ resp. $\pm w_i$ will not be distinguished. Without loss of generality we can fix the constellation as shown in figure 1.[5] The tiles of the icosahedral tilings are the projections of the 3-dimensional faces of the 6-dimensional unit cube C^6 onto E. In other words: the tiles are built by the span of three linearly independent vertex vectors of an icosahedron in the projection space E. But how many of such combinations of vertices are possible? Concerning this we have to take a look at the icosahedron

---

[2] Choose any four different indices $i, j, k, l \in \{1, \ldots, 6\}$. For any four integers $p, q, r, s \in \mathbb{Z}$ let $A_{pqrs} = \{x \in \mathbb{R}^6 : x_i = p + \frac{1}{2}, \, x_j = q + \frac{1}{2}, \, x_k = r + \frac{1}{2}, \, x_l = s + \frac{1}{2}\}$ and $B_{pqrs} = \pi_F(A_{pqrs})$. Then A_{pqrs} intersects $E_o + b$ precisely for $b \in B_{pqrs}$. If we choose $a \in F$ outside the countably many planes $B_{pqrs} \subset F$, for any $p, q, r, s \in \mathbb{Z}$ and any combination of four different indices i, j, k, l, then no point $x \in E = E_o + a$ can have four coordinates in $\mathbb{Z} + \frac{1}{2}$.

[3] In the following we do not distinguish between the terms *tiling* and *vertex set*, cf. theorem 3.5.

[4] The two different 3-dimensional irreducible representations of the icosahedral group G differ by an outer automorphism of A_5.

[5] In figure 1 we see that $U(v_6) = v_1 + v_2 + v_3 + v_4 + v_5$. On the other hand, $U(v_6) = \sqrt{5}v_6$, cf. theorem 2.1. Therefore $v_1 + v_2 + v_3 + v_4 + v_5 = \sqrt{5}v_6$.
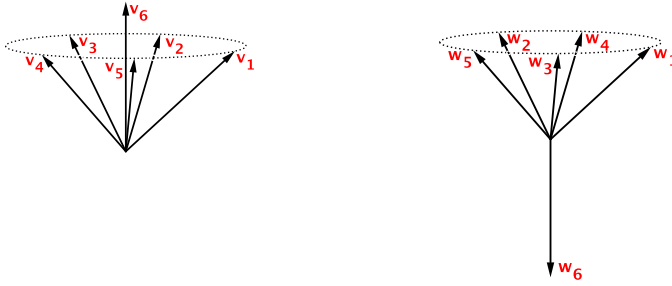
Figure 1. Left the projection of the basis vectors $e_1, \ldots, e_6$ onto E and right the projection of the basis vectors onto F

and the different relations between its vertices, cf. figure 2. For the vertex 6, three types of neighbours exist: the *direct neighbours* $1, 2, 3, 4, 5$, the *indirect neighbours* $-1, -2, -3, -4, -5$, and the *antipodal vertex* -6. Therefore two arbitrary linearly independent basic vectors v and v' with $v, v' \in \{\pm v_1, \ldots, \pm v_6\}$ are either direct or indirect neighbours of the icosahedron. They always span a *golden rhomb*[6], denoted by $R(v, v')$ in the following.
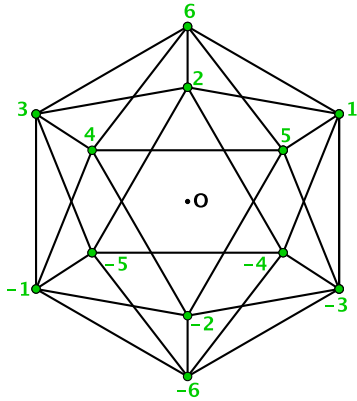

Figure 2. Vertex labelling

Altogether there are four different types of linearly independent vertices

1. Three pairwise direct neighbours, e. g. $1, 5, 6$
2. Two direct neighbours and an indirect neighbour, e. g. $1, 2, 5$
3. Two indirect neighbours and a direct neighbour, e. g. $1, 3, 4$
4. Three pairwise indirect neighbours, e. g. $1, -2, 3$

and we obtain two different types of tiles: a *flat tile* and a *long tile*. Both are equilateral rhombohedra with golden rhombs as faces, see figure 3.[7] The vertices of the flat tile are of type 2 (for the acute vertex) and 4 (for the obtuse vertex) while for the long tile the vertices are of type 1 (acute) and type 3 (obtuse).

---

[6]This is a rhomb with diagonals in golden ratio proportion. Of course, the analogous statement also holds for two arbitrary linearly independent vectors $w, w' \in \{\pm w_1, \ldots, \pm w_6\}$.
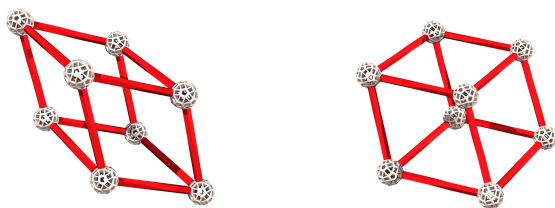[7]By courtesy of Paul Hildebrandt, Zoometool Inc.

Figure 3. Left the long tile and right the flat tile [7]

Below a schematic representation of the tiles will be important. In figure 4 we have drawn a planar projection of the six vertices of a half icosahedron (plus five antipodal vertices in the right figure), and each coloured edge corresponds to the rhomb spanned by two vertex vectors in 3-space.
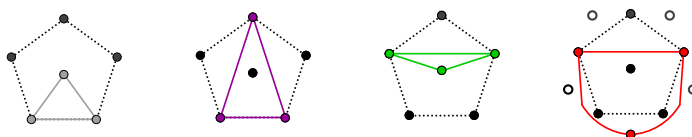

Figure 4. From left to right: long tile, seen from its acute vertex (yellow) and from its obtuse vertex (purple), as well as the flat tile, seen from its acute vertex (green) and from its obtuse vertex (red)

Using the orthogonal space F we have an alternative characterization of the 6-dimensional strip $\Sigma = E + C^6$ which serves to reduce the considered dimensions from six to three. It is called *window* $V \subset F$ and it satisfies

$$\Sigma = E + C^6 = E + V \quad \text{with } V := \pi_F(C^6) \tag{2.9}$$

Being a projection onto F of the convex unit cube C^6, the window V itself is convex and it is bounded by the projections of the 2-dimensional faces of C^6. These projections are spanned by linearly independent vectors w and w' with $w, w' \in \{\pm w_1, \ldots, \pm w_6\}$ which form always a golden rhomb, cf. footnote 6. Since there are $\binom{6}{2} = 15$ pairs of linearly independent vectors w and w' we obtain 15 parallel classes of golden rhombs. By convexity of the projection, parallel rhombs always come in pairs, cf. proof of lemma 6 in the appendix, and therefore the window V is a rhombic triacontahedron: a convex equilateral polyhedron bounded by 30 golden rhombs with 32 vertices and 60 edges, see figure 5.[9]

---

[8]By courtesy of Paul Hildebrandt, Zoometool Inc.

[9]The rhombic triacontahedron was discovered and named by Johannes Kepler, [11], [12, p. 62], https://archive.org/stream/ioanniskepplerih00kepl#page/n85/
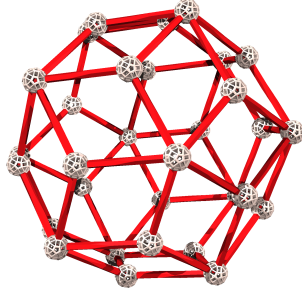
Figure 5. The window V in the orthogonal space F [8]

But the window V is more than just a lower dimensional substitute for the strip; it distinguishes which integer vectors $z \in \mathbb{Z}^6$ are admissible, i.e. projected to vertices of our tiling. For any grid point $z \in \mathbb{Z}^6$ let $z_E := \pi_E(z)$ and $z_F := \pi_F(z)$. Then[10]

$$z_E \text{ belongs to } M_E$$
$$\Longleftrightarrow z \text{ is projected onto } E$$
$$\Longleftrightarrow z \in (E + C^6) \subset \mathbb{R}^6 \tag{2.10}$$
$$\Longleftrightarrow z_F \in V$$

Using the linearity of the projection we can apply these equivalences also to the neighbour points[11] of the grid point $z \subset \mathbb{Z}^6$ which are $z \pm e_i \subset \mathbb{Z}^6$ for all $1 \leq i \leq 6$:

$$z_E \pm v_i \text{ belongs to } M_E$$
$$\Longleftrightarrow z_F \pm w_i \in V \tag{2.11}$$

Thus the window V also gives a decision criterion for admissible neighbour points of an arbitrary grid point $z \subset \mathbb{Z}^6$ and it provides information about all the possible *vertex configurations* of the tiling M_E. In fact, we may ask: where in $V \subset F$ must z_F be located so that for z_E in the projection space E a certain neighbour point $z_E + v$ with $v \in \{\pm v_1, \ldots, \pm v_6\}$ is also part of the tiling M_E? By systemizing this concept we get a partition of the window V in disjoint regions and each region belongs to a certain vertex configuration, see [6].

Remark 2.2. In the following the equivalences in (2.10) and (2.11) will be important because they allow us to switch back and forth (without any loss of information) between the ambient space W on the one side and the projection space E or the orthogonal space F on the other side.

---

[10] Here we are using that the eigenspaces of U are irrational, i.e. they do not contain any nonzero integer vector, see theorem 2.1.

[11] In the present paper *neighbour* or *neighbour point* of a grid point always means another integer point one of whose coordinates differs by ± 1.
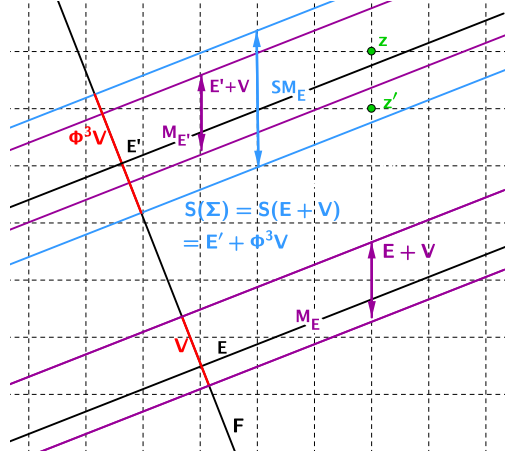
2.2. Inflation and deflation

Figure 6. The process of inflation and deflation: the projection space corresponds to the straight line E and the orthogonal space to the straight line F.

We now introduce the concept of *inflation* and its inverse, called *deflation*. By applying the linear map $S = 2I - U$ introduced in (2.4), the following situation occurs on the strip $\Sigma = E + C^6$ with $E = W_+ + a$ and $a \in F$:

$$S(\Sigma) = S(E + V) = E' + \Phi^3 V \tag{2.12}$$

since $S(E) = S(W_+ + a) = W_+ + \Phi^3 a =: E'$. The symmetric matrix S itself is integer and because of $\det S = -1$ also integer invertible. Therefore we obtain two different tilings on the parallel subspace E'. The tiling

$$SM_E := \pi_{E'}\big(\mathbb{Z}^6 \cap S(\Sigma)\big) = \pi_{S(E)}\big(S(\mathbb{Z}^6 \cap \Sigma)\big) \tag{2.13}$$

as well as the tiling

$$M_{E'} = \pi_{E'}(\mathbb{Z}^6 \cap \Sigma') \tag{2.14}$$

where $\Sigma' := E' + C^6$. What is the relation between the tiling M_E on the subspace E and the tilings $M_{E'}$ and SM_E on the shifted subspace E'?

Theorem 2.3. *The tiling SM_E is a proper refinement of $M_{E'}$, i.e. $M_{E'} \subset SM_E$.*

Proof. $\Sigma' \subset S(\Sigma)$ because the transformed strip $S(\Sigma)$ is by the factor Φ^3 larger than the usual strip Σ'. With (2.13) and (2.14) we observe

$$M_{E'} = \pi_{E'}(\mathbb{Z}^6 \cap \Sigma') \subset \pi_{E'}\big(\mathbb{Z}^6 \cap S(\Sigma)\big) = SM_E.$$

$\square$

Theorem 2.4. *The tiling SM_E is homothetic to the tiling M_E. More precisely: SM_E is an image of M_E, point reflected and scaled-down by the factor φ^3.*

Proof. By definition the subspace E is a translated eigenspace of S and hence $S \circ \pi_E = \pi_E \circ S$, which means that we can also first project and then apply S. Because of (2.1) and (2.13) we have

$$SM_E = \pi_{S(E)}\big(S(\mathbb{Z}^6 \cap \Sigma)\big) = S\big(\pi_E(\mathbb{Z}^6 \cap \Sigma)\big) = S(M_E)$$

with $M_E \subset E$ and S has eigenvalue $-\varphi^3$ in the direction of E. $\square$

This shows the *inflation property* of the tiling, see figure 6: the vertex set SM_E which is a homothetic image of M_E has $M_{E'}$ as a subset. Thus the vertex set $M_{E'}$ can be extended to the vertex set of another icosahedral tiling whose tiles are smaller by the factor φ^3. Therefore we call $M_{E'}$ *inflation tiling* or *coarse tiling* of SM_E and the linear transformation S also *inflation map*. The inverse of this procedure is called *deflation*: the tiling SM_E is the *deflation tiling* or *fine tiling* of $M_{E'}$ and $T := S^{-1}$ the *deflation map*, see [8]. The vertices of $M_{E'}$ will also be called *old vertices*. Thereby the following question arises: what happens to the coarse tiles of $M_{E'}$ under deflation? For the Penrose tilings of the plane the procedure of deflation is defined in such a way that every coarse tile has the same subdivision, cf. [5], but does the subdivision of the tiles also occur in an unique way in the case of icosahedral tilings in space?

Figuring out this problem the following idea is necessary: let $z \in \mathbb{Z}^6$ be a point inside the strip $\Sigma' \subset S(\Sigma)$ then $z_{E'} := \pi_{E'}(z)$ belongs to the coarse tiling $M_{E'}$ as well as to the fine tiling SM_E. But viewing $z_{E'}$ as an element of $M_{E'}$ it has another vertex configuration than when we view it as an element of SM_E.[12] Therefore understanding the procedure of deflation involves to figure out the connection between the old vertex configuration of $z_{E'}$ in $M_{E'}$ and the new vertex configuration of $z_{E'}$ in SM_E. Because SM_E is homothetic to the tiling M_E on the subspace E, cf. theorem 2.4, we can answer this question by studying the connection between $M_{E'}$ and M_E. Hence we may use the deflation map $T = S^{-1}$ and we have to investigate what happens to the window V under T.

3. Deflation in the case of the icosahedral tilings

We adopt the terminology introduced in 2.1 and 2.2. Let $z_{E'}$ always denote an arbitrary old vertex of the coarse tiling $M_{E'}$ in the projection space E' then $z_{F'}$ denotes the corresponding point in the orthogonal space F, cf. remark 2.2. If $z_{E'}$ resp. $z_{F'}$ has j neighbour points then $z_{E'}$ resp. $z_{F'}$ is called *vertex of type ω_j*.[13]

---

[12]See figure 6: for $z \subset (E' + C^6) \subset (E' + SC^6)$ we have $z' \not\subset (E' + V)$, but $z' \subset (E' + \Phi^3 V)$; i.e. $z_{E'}$ belongs not to the coarse tiling $M_{E'}$, however $z_{E'}$ is an element of the fine tiling SM_E.

[13]Of course j can be specified; in the case of icosahedral tilings it is $j \in \{4, 5, 6, 7, 8, 9, 10, 12\}$, see [6]. Because for $1 \leq i \leq 6$ the basic vectors $\pm v_i$ point to the vertices of an icosahedron in a different configuration than the basic vectors $\pm w_i$, cf. figure 1 and footnote 4, a vertex of type ω_j can have another shape in the projection space E than in the orthogonal space F, cf. figure 10.

Concerning the question of a possible subdivision of the tiles we proceed step by step. We first examine: what happens to all old vertices under deflation?

3.1. Subdivision at vertices

Theorem 3.1. *All vertices $z_{E'}$ of the coarse tiling $M_{E'}$ turn into vertices of type ω_{12} with respect to the fine tiling SM_E.*

Proof. The deflation factor is $\varphi^3 = \sqrt{5} - 2$ and therefore the deflation map T shrinks the window V by exactly this factor. According to the equivalences in (2.10) and (2.11) we have to ask: for which basic vector w with $w \in \{\pm w_1, \ldots, \pm w_6\}$ we have

$$\varphi^3 V + w \subset V \,? \tag{3.1}$$

Consider the homothetic map $h : x \mapsto \varphi^3 x + w$.[14] Its scale factor is φ^3 and for the fixed point y we obtain $y = \frac{1}{1-\varphi^3}\, w$. Concerning lemma 1 in the appendix we have to verify

$$y \subset V \quad \text{for each } w \in \{\pm w_1, \ldots, \pm w_6\} \tag{3.2}$$

then (3.1) holds for all $w \in \{\pm w_1, \ldots, \pm w_6\}$ satisfying (3.2). Since $\frac{1}{1-\varphi^3} = \frac{\Phi^3}{\Phi^3-1} = 1 + \frac{1}{2}\varphi$ (recall that $\Phi^2 = \Phi + 1$ and hence $\Phi^3 = \Phi^2 + \Phi = 2\Phi + 1$) and $\Phi = 1 + \varphi$, we have $\frac{1}{1-\varphi^3} < \Phi$.

Because Φw is a vertex of the window V for all $w \in \{\pm w_1, \ldots, \pm w_6\}$, the scaled down window $\varphi^3 V$ can be shifted in any direction of the 12 basic vectors $\pm w_i$ for all $1 \leq i \leq 6$ without leaving the original window V.[15] Thus all old vertices $z_{E'}$ of the coarse tiling $M_{E'}$ turn into vertices of type ω_{12} in the fine tiling SM_E. $\qquad\square$

Condition (3.1) can be illustrated by considering the projection image of the window V, see figure 7.[16] From theorem 2.3 it is known that the tiles of the fine tiling SM_E are by the factor φ^3 smaller than the tiles of the coarse tiling $M_{E'}$. By construction the tiles of $M_{E'}$ are spanned by the basic vectors $\pm v_1, \ldots, \pm v_6$, therefore the tiles of the fine tiling SM_E are spanned by the reduced basic vectors $\pm \varphi^3 v_1, \ldots, \pm \varphi^3 v_6$ and in terms of the fine tiling SM_E we also call $\pm \varphi^3 v_1, \ldots, \pm \varphi^3 v_6$ *basic vectors*. The situation can be illustrated as shown in figure 8. Concerning the question of a possible subdivision of the coarse tiling $M_{E'}$ we have to do a further step: what about the neighbours of the old vertices in the fine tiling SM_E? Which vertex configurations are possible for them?

---

[14]It is $h = t \circ h'$ where $h' : x \mapsto \varphi^3 x$ is a homothety and $t : x \mapsto x + w$ is a translation. Such composition is a homothetic map with a different center.

[15]The vertices of the window V are projections of the vertices of the 6-dimensional unit cube C^6 onto F. Therefore the vertices of V are sums built by $\pm w_1, \ldots, \pm w_6$, cf. page 6. But not all of these $2^6 = 64$ possible sums span the convex polyhedron V. Altogether there are two types of *maximal sums*, i.e. sums not lying inside the window but building a vertex of V: the maximal sum Φw with $w \in \{\pm w_1, \ldots, \pm w_6\}$ pointing to the 12 vertices of an icosahedron and the maximal sum pointing to the 20 vertices of a dodecahedron, see [6].

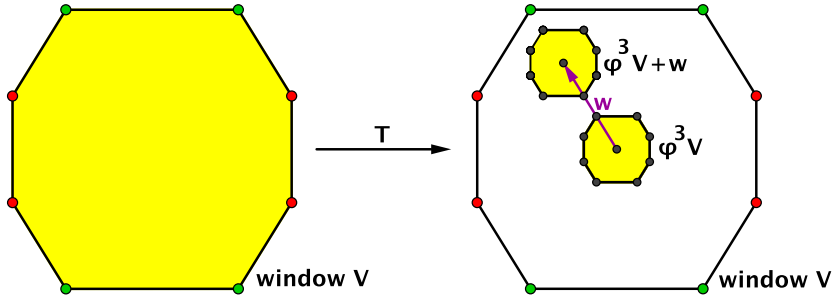[16]As the projection plane we always choose the plane of a rhomb of the window V.

Figure 7. The window V under the deflation map T

(a) flat tile   **(b)** long tile
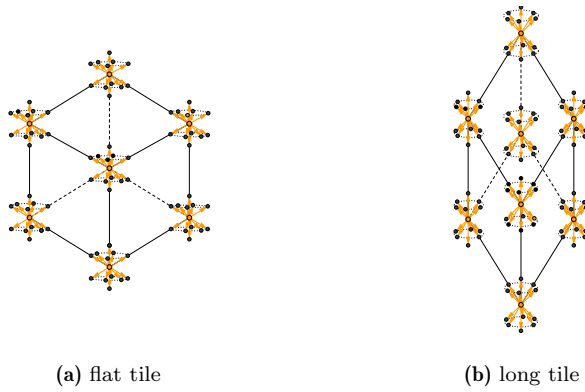
Figure 8. Transformation of the vertices of the coarse tiling $M_{E'}$ into vertices of type ω_{12} in the fine tiling SM_E

For $v \in \{\pm v_1, \ldots, \pm v_6\}$ the neighbour point $z_{E'} + \varphi^3 v$ of an arbitrary old vertex $z_{E'}$ in the fine tiling SM_E is named *first neighbour*.

Theorem 3.2. *The first neighbours of all old vertices $z_{E'}$ in the fine tiling SM_E are vertices of type ω_6 and look like flowers in the projection space E'.*

More precisely: the edge between an old vertex $z_{E'}$ and its first neighbour always builds the flower stalk, the five remaining basic vectors form the petals.

Proof. From theorem 3.1 it is known that in the fine tiling SM_E the old vertex $z_{E'}$ is a vertex of type ω_{12}. In order to find out the type of vertex for the first neighbours of $z_{E'}$ we have to ask: for which vectors w and w' with $w, w' \in \{\pm w_1, \ldots, \pm w_6\}$ we have

$$\varphi^3 V + w + w' \subset V \, ? \tag{3.3}$$

Considering the symmetry of the icosahedron the basic vectors w and w' can be related in four different ways:

1. If $w' = -w$ we obtain the trivial case $\varphi^3 V \subset V$ and condition (3.3) holds naturally.
2. If w' is a indirect neighbour of w then $w + w'$ is the short diagonal of $R(w, w')$ and the proof is as given in theorem 3.1. In this case we consider the homothety $h : x \mapsto \varphi^3 x + w + w'$. Its fixed point is $y = \frac{1}{1-\varphi^3}(w + w')$ and $w + w'$ now points to the direction of the midpoint of the faces of the rhombic triacontahedron, see figure 9. But we still obtain $y \subset V$ and therefore condition (3.3) holds for all indirect neighbours w' of w.
3. If w' is a direct neighbour of w then $w + w'$ is the long diagonal of $R(w, w')$. By planar geometry considering the projection image of V we can prove that condition (3.3) fails for all direct neighbours w' of w, see figure 9. In each case we have to choose the projection plane parallel to the two pairs of basic vectors $\pm w$ and $\pm w'$. Then the translation of the reduced window $\varphi^3 V$ to $w + w'$ is mapped isometrically and we obtain $(\varphi^3 V + w + w') \cap V = \emptyset$.
4. If $w' = w$ we can apply the proof given in case 3, see figure 9. It follows $(\varphi^3 V + 2w) \cap V = \emptyset$ and therefore also in this case condition (3.3) fails.
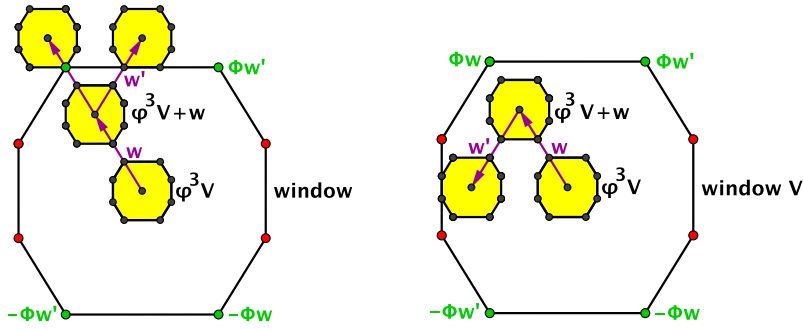

Figure 9. Shifting $\varphi^3 V + w$ to w' is not admissible if w' is a direct neighbour of w or if $w' = w$, see left figure. The right figure illustrates case 2 where w' is a indirect neighbours of w.

Therefore in the projection space E' an arbitrary first neighbour $z_{E'} + \varphi^3 v$ of any old vertex $z_{E'}$ always has the neighbour points

$$z_{E'} + \varphi^3 v - \varphi^3 v = z_{E'} \quad \text{and} \quad z_{E'} + \varphi^3 v + \varphi^3 v' \tag{3.4}$$

where $v \in \{\pm v_1, \ldots, \pm v_6\}$ and v' is a direct neighbour of v, cf. the equivalences in (2.10) and (2.11).[17] We call this type of vertex ω_6. Because of its shape in the projection space E' we also call it *flower (vertex)*, see figure 10. □
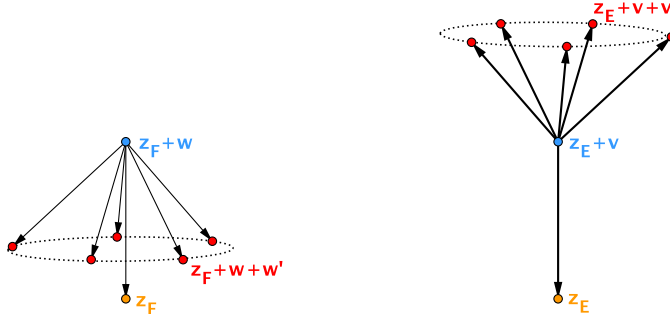

Figure 10. A vertex of type ω_6 in the orthogonal space F and in the projection space E

Moreover we also know which tiles surround each flower stalk:

Theorem 3.3. *The flower stalk of any vertex of type ω_6 is surrounded by five long tiles.*

Proof. Fixing the first neighbour $z_{E'} + \varphi^3 v_6$, we may ask: which tiles surround the edge between $z_{E'}$ and $z_{E'} + \varphi^3 v_6$? Because all first neighbours of $z_{E'}$ in the fine tiling SM_E are vertices of type ω_6 we know that the blue marked edges in figure 11 (left) exist.

As a result we obtain the rhombs $R(1,5), R(1,6), R(5,6)$.[18] These three rhombs are pairwise non-parallel and they form a long tile.[19] With the same arguments four further long tiles exist around the edge between $z_{E'}$ and $z_{E'} + \varphi^3 v_6$ and hence we get the situation shown in figure 11 (right). For the sake of clarity just three of the five long rhombs are shown. The same considerations can be made for all other first neighbours of $z_{E'}$ and theorem 3.3 is proved.

□

Directly from theorem 3.3 we obtain:

Theorem 3.4. *The petals of any flower span a blossom of five rhombs.*

---

[17]In (3.3) we investigate the tiling M_E, homothetic to the fine tiling SM_E, cf. theorem 2.4. Transferring results from M_E to SM_E which are not invariant under similarity transformations therefore needs to apply S and therefore v' is now a direct (not indirect) neighbour of v.

[18]For the sake of brevity the first neighbour $z_{E'} \pm \varphi^3 v_k$ is denoted by $\pm k$ for $1 \le k \le 6$

[19]The 3D-tiling induces a 2D-tiling on the sphere S around each vertex. The three rhombs $R(1,5), R(1,6), R(5,6)$ intersect S in three edges of the 2D-tiling bounding a triangle in S. This is the intersection of S with a 3d-tile. Thus these three rhombs bound a common (long) tile.

Proof. In figure 11 we see: two neighbouring petals of any flower span a rhomb. Because each flower has five petals we obtain a *blossom* of altogether five rhombs.
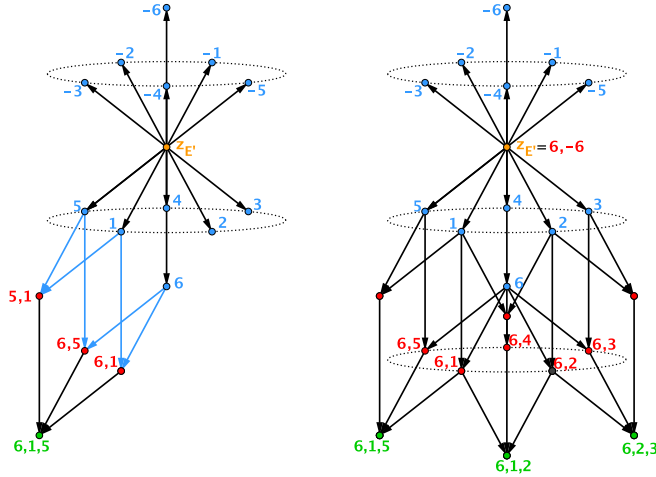
$\square$

Figure 11. The long tiles around $z_{E'}$ and $z_{E'} + \varphi^3 v_6$ in the fine tiling SM_E, the notation is according to footnote 18

Therefore an arbitrary old vertex $z_{E'}$ of the coarse tiling $M_{E'}$ is surrounded by altogether 20 long tiles in the fine tiling SM_E: according to the theorems 3.1 and 3.2 the old vertex $z_{E'}$ is a vertex of type ω_{12} in SM_E and all of its 12 first neighbours are flowers. Each stalk of these flowers is surrounded by 5 long tiles, see theorem 3.3, but three neighbouring stalks always have a long tile in common.

3.2. Subdivision along edges

3.2.1. Subdivision along edges near endpoints. Based on the results of 3.1 we obtain the situation as shown in figure 12.
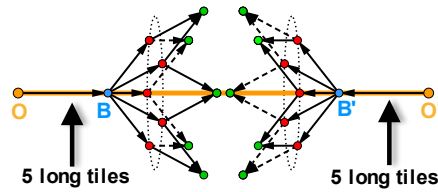

Figure 12. Unfinished subdivision of an arbitrary coarse edge

Comments on figure 12:

- A coarse edge and its endpoints, denoted by O and O', are marked orange. O and O' are both old vertices, thus they are vertices of type ω_{12} in the fine tiling SM_E, cf. theorem 3.1.
- The two blue marked points B and B' are first neighbours of O and O'. Concerning theorem 3.2 they are flowers and their flower stalks OB and $O'B'$ are both surrounded by five long tiles, cf. theorem 3.3.
- The petals of B and B' are marked red and the two blossoms spanned by them are drawn above, cf. theorem 3.4. Note that each rhomb of these blossoms is the face of one of the long tiles surrounding OB and $O'B'$.

Hence each coarse edge near its endpoints is surrounded by five long tiles in the fine tiling SM_E.

3.2.2. Subdivision along edges near midpoints. We have to close the remaining gap in figure 12. The drawn ten rhombs separate into two blossoms adjoining to the first neighbours B and B', cf. theorem 3.4. Because B and B' are antipodal points these blossoms are antipodal. Furthermore we have

$$|B - B'| = |O - O'| - 2\varphi^3|v| = |v| - 2\varphi^3|v| = \sqrt{5}\,\varphi^3|v|$$

where by construction $v \in \{\pm v_1, \ldots, \pm v_n\}$ is an edges of the coarse tiling and $\varphi^3 v$ an edge of the fine tiling SM_E. Therefore the ten rhombs in figure 12 form a *lense*[20]: a convex equilateral polyhedron bounded by 20 golden rhombs with 22 vertices and 40 edges. The following theorem guarantees the existence of the missing edges (the ten edges between the green points in figure 12):

Theorem 3.5. *If two points in the icosahedral tilings differ by an admissible edge vector then they are connected by an edge.*

Proof. Let z_{1E} and z_{2E} be two points in an arbitrary tiling M_E which differ by an admissible edge vector, i.e.

$$z_{1E} - z_{2E} = v$$

with $v \in \{\pm v_1, \ldots, \pm v_6\}$. We want to prove that the edge between z_{1E} and z_{2E} exists in fact.

For the inverse image point $z_1 = \pi_E^{-1}(z_{1E})$ in the ambient space W we have $z_1 \in (E + C^6) \subset \mathbb{R}^6$, cf. (2.10), and the admissible edge v corresponds to the unit vector $e = \pi_E^{-1}(v)$ with $e \in \{\pm e_1, \ldots, \pm e_6\}$. Moving from z_1 along e we reach the point $z_1 + e = z^*$. Because the orthogonal space F is irrational, i.e. it does not contain any nonzero integer vector, no two different grid points in W can be projected onto the same point in E. Therefore it is $z^* = z_2 = \pi_E^{-1}(z_{2E})$. But with z_1 and z_2 also the line segment between these two points lies inside the strip $\Sigma = (E + C^6) \subset \mathbb{R}^6$ since the strip is convex. Hence in the tiling M_E the edge between z_{E_1} and z_{E_2} exists. $\qquad\square$

Thus each coarse edge near its midpoint is surrounded by a lense, see figure 13.

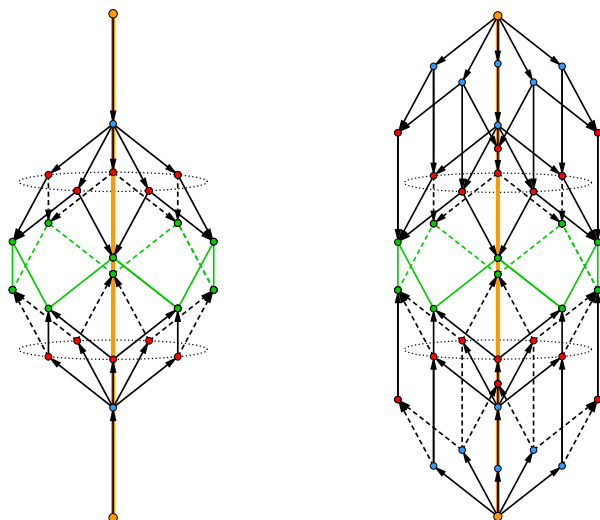[20]See comments on figure 32 and remark 4.1 in the appendix.

Figure 13. Subdivision of an arbitrary coarse edge. On the left, the lense around the middle part of the coarse edge is shown, on the right we see the lense together with the five long tiles adjoining to the lense from left and right, see 3.2.1.

We prove in the appendix, see lemma 3, that each lense can be filled with five long and five flat tiles and the filling is unique up to isometries of the lense. The question remains if all of these ten congruent fillings are realized for each of the lenses. The answer to this problem needs some more detailed knowledge, for this purpose see [6].

3.3. Subdivision of the faces

Each face of the icosahedral tiling is a golden rhomb. Transferring the results from 3.2 to the four edges of a coarse rhomb we directly obtain the subdivision of a coarse face in the fine tiling SM_E.
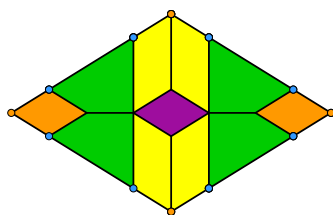

Figure 14. Subdivision of the face

Comments on figure 14:

- Each of the four vertices of the coarse rhomb, marked orange, is surrounded by 20 long tiles in fine tiling SM_E. The intersection of these long tiles with the coarse rhomb depends on whether the two coarse edges at the old vertex are direct or indirect neighbours in the icosahedron, cf. page 6.
  - If the coarse edges are direct neighbours then the intersection is a golden rhomb, more precisely a face of the fine tiling SM_E, orange marked.
  - If the coarse edges are indirect neighbours then the intersection contains the diagonal and has the shape of a certain parallelogram, yellow marked, cf. figure 22 below
- Each coarse edge near its midpoint is surrounded by a lense, see 3.2.2. The four green marked quadrangles are the intersections of these lenses with the coarse rhomb.
- In the center of the coarse rhomb the four yellow marked rhombs just enclose a further golden rhomb, purple marked[21]

3.4. Subdivision of the tiles

We obtain the situation as shown in figure 15. For both tiles the lenses 1 to 6 are called *inner lenses*, accordingly the lenses 7 to 12 are also called *outer lenses*. Also the corresponding edges will be named *inner* and *outer* edges, accordingly. The following two questions remain:

1. Which of the 20 long tiles surrounding each old vertex, cf. 3.1, belong to the coarse tiles?
2. What about the interior part of the coarse tiles (long and flat)?
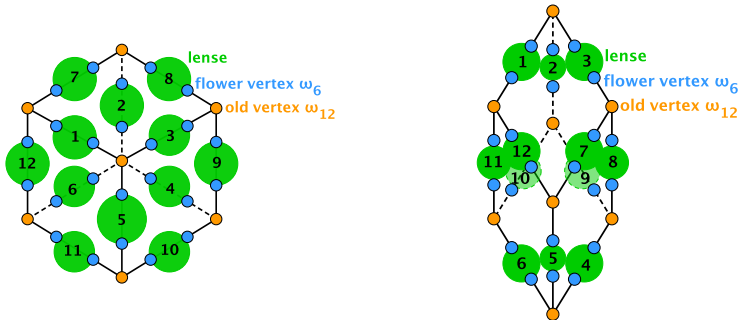

Figure 15. Subdivision of the edges of an arbitrary coarse tile: left the flat and right the long tile. For the sake of clarity the five long tiles always adjoining to the lenses from left and right are not shown.

---

[21] The four edges enclosing a rhomb actually bound a face of the tiling since they are projected from an admissible square in the lattice $\mathbb{Z}^6$, see proof of theorem 3.5.

3.4.1. Subdivision of the flat tile.

Long tiles inside the coarse flat tile. The first question can be answered by considering the schematic representation of the vertices of the tiles, cf. figure 4. In figure 16 we see the six vertices of an icosahedron lying in a common half space (marked dark bold) and five antipodal vertices. Only the antipodal vertex of the bold marked vertex in the center is invisible. Assuming that the bold marked vertex in the center is an old vertex $z_{E'}$, figure 16 shows 15 of the 20 long tiles surrounding $z_{E'}$.
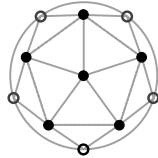

Figure 16. 15 of the 20 possibilities to build a long tile in SM_E arising from $z_{E'}$.

Theorem 3.6. *At the two obtuse vertices always four whole long tiles and six half long tiles (belonging to the fine tiling SM_E) lie inside the coarse flat tile. At the six acute vertices always two half long tiles of the fine tiling SM_E lie inside the coarse flat tile.*

Figure 17. Left the schematic representation of an obtuse vertex of the flat tile, right an acute vertex of the flat tile always together with 15 of the 20 possibilities to build a long tile seen from its acute vertex

Proof. **Comments on figure 17:**
- Three vertices of an icosahedron which together span a flat tile seen from its obtuse vertex are marked red, three vertices of an icosahedron which together span a flat tile seen from its acute vertex are marked green.
- Yellow marked are always 15 of the 20 possibilities to build a long tile seen from its acute vertex.
- Therefore in the left figure the four triangles highlighted in yellow correspond to long tiles at an obtuse vertex lying completely inside the coarse flat tile and the six numbered triangles correspond to long tiles lying half inside the coarse flat tile.

- Similarly, in the right figure the two triangles highlighted in yellow correspond to long tiles at an acute vertex lying half inside the coarse flat tile.

□

The interior part. The two obtuse vertices of the coarse flat tile are close to each other. This fact leads to the following result:

Theorem 3.7. *The two obtuse vertices of the coarse flat tile are connected by a long tile of the fine tiling SM_E.*

Proof. In the appendix, lemma 4, we prove that the ratio of the long diagonal of the long tile and the short diagonal of the flat tile corresponds to Φ^3. Since the deflation factor of the icosahedral tilings is also Φ^3 the length of the short diagonal of a coarse flat tile corresponds to the length of the long diagonal of a fine long tile. According to 3.1 each old vertex of the coarse tiling $M_{E'}$ is surrounded by 20 long tiles in the fine tiling SM_E. One of them is pointing straight inward. Therefore the two obtuse vertices of the coarse flat tile are connected by a long tile in SM_E.   □

Remark 3.8. This long tile of the fine tiling SM_E connecting the two obtuse vertices of the coarse flat tile is also called *transversal tile*.

With the help of the transversal tile the question of the interior part of the coarse flat tile can be finally answered, see figure 18. We obtain:

Theorem 3.9. *The interior part of the coarse flat tile is filled by 7 whole and 12 half long tiles as well as 6 whole flat tiles of the fine tiling SM_E.*
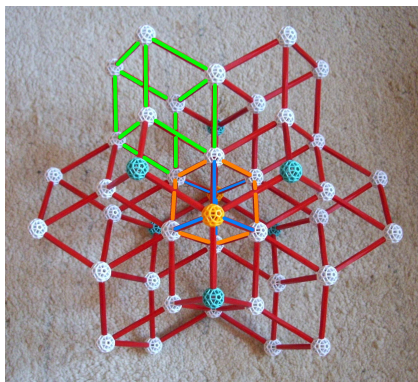
Proof.

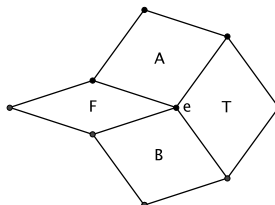**Figure 18.** Inner part of the coarse flat tile

Figure 19. Long tiles A, B adjacent to transversal tile T at edge e are connected by a flat tile F (projection plane $e^{\perp}$)

Comments on figure 18:

- The two orange vertices in the center (the second one is underneath) are the two obtuse vertices of the coarse flat tile, the blue vertices are their first neighbours in the direction of the edges of the coarse flat tile.
- The edges of the transversal tile in the center are marked blue and orange. The six blue marked edges are all flower stalks. In view of theorem 3.3,[22] we obtain six long tiles, which adjoin to the six faces of the transversal tile and lie completely inside the coarse flat tile, and twelve long tiles lying just half inside the coarse flat tile. For the sake of clarity the half-tiles are not shown in figure 18 we obtain six long tiles, which adjoin to the six faces of the transversal tile and lie completely inside the coarse flat tile, and twelve long tiles lying just half inside the coarse flat tile.
- There are two triples of long tiles adjacent to the 3+3 faces of the transversal tile T (3 on each end). Two tiles A, B belonging to different triples and sharing an edge e, one of the 6 "outer" (middle) edges of T, are connected by a flat tile, see figure 19 which is a projection into the plane perpendicular to e.

$\square$

Hence the subdivision of the coarse flat tile is known and we can calculate the number of fine tiles subdividing the coarse flat tile. Note that this is not a subdivison by whole tiles but by parts of tiles (in fact by tenths) since some fine tiles are cut into pieces by the walls of the coarse tile. However, recollecting the pieces we obtain the following integers (in fact Fibonacci numbers):

Theorem 3.10. *Any flat tile of the coarse tiling $M_{E'}$ is filled altogether by 34 long and 21 flat tiles of the fine tiling SM_E, more precisely, by 340 tenths of a long tile and 210 tenths of a flat tile.*

Proof. Each of the inner lenses takes part of the coarse flat tile by the ratio $\frac{2}{5}$, each of the outer lenses by the ratio $\frac{1}{10}$. This is seen by projecting the coarse tile into the plane perpendicular to the edge carrying the lense. The projection of a flat tile into the plane perpendicular to any of its edges is always a rhomb with angles $\frac{1}{10} \cdot 2\pi$ and $\frac{2}{5} \cdot 2\pi$, see figure 19. Thus the coarse tile cuts out a fraction of $\frac{1}{10}$ from the lenses sitting on an outer edge and $\frac{2}{5}$ from those on the inner edges. Therefore denoting the long tiles by L and the flat tiles by F we obtain for the number of tiles, using the theorems 3.6, 3.9 and Lemma 3 of the Appendix:

$$\underbrace{6\left(2 \cdot \frac{1}{2}L\right)}_{\text{acute vertices}} + \underbrace{\left(7 + \frac{12}{2}\right)L + 6F}_{\text{interior part}} + \underbrace{6\left(\frac{1}{10}(5L+5F)\right)}_{\text{outer lenses}} + \underbrace{6\left(\frac{2}{5}(5L+5F)\right)}_{\text{inner lenses}} = 34L + 21F.$$

---

[22]Each stalk is surrounded by five long tiles: the transversal tile and four further long tiles. Two of these are directly adjacent to the transversal tile and lie completely inside the coarse flat tile; in fact, each of those belong to two different flower stalks. The other two long tiles lie just half inside the coarse tile. Hence altogether we obtain six whole long tiles and twelve half long tiles inside the coarse flat tile.

□

3.4.2. Subdivision of the long tile.

Long tiles inside the coarse long tile. Also in this case we first want to examine which of the 20 long tiles of the fine tiling SM_E surrounding each old vertex lie inside the coarse long tile.

Theorem 3.11. *At the six obtuse vertices always one whole long tile and four half long tiles (belonging to the fine tiling SM_E) lie inside the coarse long tile. At the two acute vertices always one whole long tile of the fine tiling SM_E lies inside the coarse long tile.*

Proof.

Figure 20. Left the schematic representation of an obtuse vertex of the long tile, right an acute vertex of the long tile always together with 15 of the 20 possibilities to build a long tile seen from its acute vertex

Comments on figure 20:

- Three vertices of an icosahedron which together span a long tile seen from its obtuse vertex are marked purple, three vertices of an icosahedron which together span a long tile seen from its acute vertex are marked orange.
- Yellow marked are always 15 of the 20 possibilities to build a long tile seen from its acute vertex.
- Therefore in the left figure the triangle highlighted in yellow corresponds to a long tile at an obtuse vertex lying completely inside the coarse long tile and the four numbered triangles correspond to long tiles lying half inside the coarse long tile.
- Similarly, in the right figure the triangle highlighted in yellow corresponds to a long tile at an acute vertex lying completely inside the coarse long tile.

□

The interior part. The question of filling the interior part must be answered in two steps. We first examine the shape of the interior part.
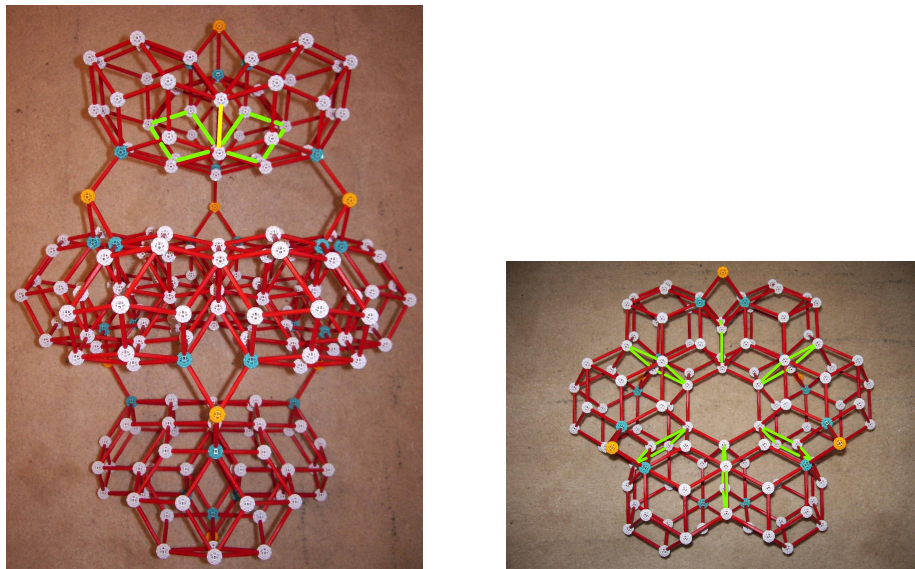

Figure 21. Left the connection between three of the inner lenses, right the outer lenses of the long tile rotated by $90°$ and isolated from the rest of the tile

Comments on figure 21:

- The inner lenses 1,2,3 and 4,5,6 pairwise share a rhomb. For example: lense 2 has a rhomb (marked green) in common with lense 1 and lense 3. Lense 1 and lense 3 also share a rhomb, but being perpendicular to the viewing direction we just see the edge marked yellow, see left figure.
- The outer lenses of the long tile form a *ring of lenses*, see right figure. Each outer lense shares a rhomb with both of its neighbour lenses, marked green.

Considering the results from 3.1 to 3.3 we obtain:

Theorem 3.12. *The interior part of the coarse long tile has the shape of two intersecting rhombic triacontahedra intersecting in a flat tile of the fine tiling SM_E.*

Proof. We investigate the cross section along the long diagonal of the coarse long tile, perpendicular to one of the faces:
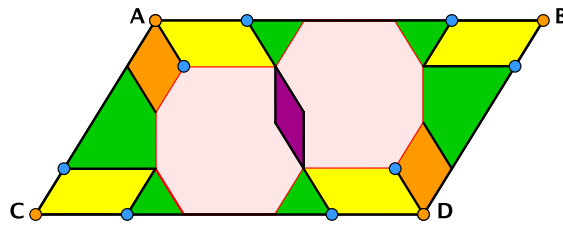
Figure 22. The cross section of the interior part

Comments on figure 22:

- The "edges" AB and CD are both long diagonals of a coarse rhomb, while AC and BD are edges of a coarse rhomb
- The four orange marked vertices of the cross section are old vertices
- The yellow parallelograms and the orange rhombs are the long tiles surrounding any old vertex, the lenses are marked green
- The drawn rhombs and lenses enclose a pink marked gap. It has the shape of two intersecting rhombic triacontahedra intersecting in a flat tile of the fine tiling SM_E, marked purple, cf. footnote 21

$\square$

In a second step we ask: which tiles of the fine tiling SM_E fill these intersecting rhombic triacontahedra? For a better understanding we first have to get in touch
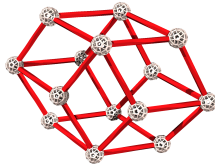

Figure 23. Minilense [23]

with another convex equilateral polyhedron. We call it *minilense* and it is bounded by 12 golden rhombs with 14 vertices and 24 edges, see figure 23. With the help of the minilenses it is possible to construct an invariant structure inside the two intersecting rhombic triacontahedra of the coarse long tile.

Theorem 3.13. *The interior part of the coarse long tile is subdivided by an invariant structure consisting of seven flat and eight long tiles and six minilenses in the fine tiling SM_E.*

---

[23]By courtesy of Paul Hildebrandt, Zoometool Inc.

Proof. The considerations made in 3.1 and 3.2 have been too coarse in some sense: in order to investigate what happens to an arbitrary coarse long tile under deflation we actually don't have to work with the whole window V.

Excursus 1
Let z_E be a point of an arbitrary tiling M_E in the projection space E and assume that z_E is an acute vertex of a long tile with edge vectors v_i, v_j, v_k.[24] Therefore besides z_E also the seven remaining vertices of that long tile must belong to the tiling M_E, i.e. the points $z_E + v$ for $v \in \{v_i, v_j, v_k, v_i + v_j, v_i + v_k, v_j + v_k, v_i + v_j + v_k\}$. According to the equivalences in (2.10) and (2.11) we observe the following conditions for the corresponding point z_F in the orthogonal space F:

(i) $z_F \in V$

(ii) $z_F + w \in V$ for $w \in \{w_i, w_j, w_k, w_i + w_j, w_i + w_k, w_j + w_k, w_i + w_j + w_k\}$

Let $\Omega_{(i,j,k)}$ be the part of the window V satisfying the conditions (i) and (ii). Then we obtain

$$z_F \in \Omega_{(i,j,k)} \iff \text{from } z_E \text{ arises a long tile by } v_i, v_j, v_k \qquad (3.5)$$

$\Omega_{(i,j,k)}$ itself has the shape of a long tile, see lemma 5 in the appendix. According to the 20 possibilities of choosing three pairwise direct icosahedral neighbours, cf. footnote 24, there are altogether 20 congruent regions inside the window V realizing a long tile from its acute vertex. Each of these regions is also called *region of type* Ω.[25]
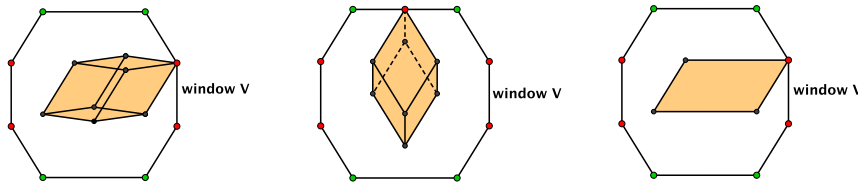

Figure 24. From left to right three illustrations of the region of type Ω: perspective, projection and cross section

From excursus 1 it follows: let $z_{E'}$ be an old vertex of the coarse tiling $M_{E'}$ and assume that from $z_{E'}$ arises a coarse long tile from its acute vertex by the basic vectors v_i and v_j as well as v_k. Then it holds true

$$z_{F'} \in \Omega_{(i,j,k)} \qquad (3.6)$$

---

[24]In that case v_i, v_j, v_k are pairwise direct icosahedral neighbours. Altogether there are 20 possible combinations for three pairwise direct neighbours in the icosahedron.

[25]Of course the same considerations can be made for the long tile seen from its obtuse vertex and the flat tile seen from its acute or obtuse vertex. The corresponding regions in the window V always have the same shapes as the tiles we are starting from, cf. lemma 5 in the appendix.

for the corresponding point $z_{F'}$ in the orthogonal space F and $\Omega_{(i,j,k)}$ is the part of V we have to work with. Hence concerning the question what happens to the long tile under deflation the following steps are neccessary:

1. Apply the deflation map T to the region $\Omega_{(i,j,k)}$
2. Find the region of the window V in which the image of $\Omega_{(i,j,k)}$ under T lies
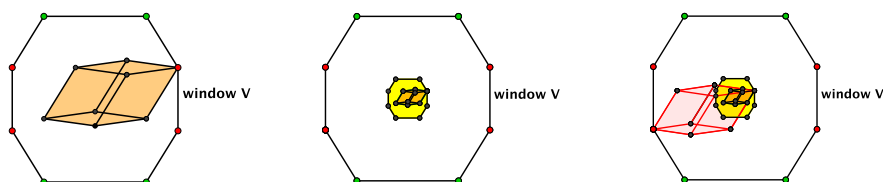3. Apply S to the results of step 2, cf. footnote 17

Figure 25. Illustration of the steps 1 to 3, where $\Omega_{(i,j,k)}$ is marked orange

Figure 25 illustrates the steps 1 to 3: applying T to $\Omega_{(i,j,k)}$ (left) means to reduce it by the factor φ^3 (middle) and the reduction lies inside a certain red marked region (right). In order to figure out what it is about this region it is necessary to investigate more about the window V and its different regions. All in all we register

$$z_{F'} \in \varphi^3(\Omega_{(i,j,k)}) \subset \text{red marked region} \qquad (3.7)$$

Excursus 2

Again let z_E be part of an arbitrary tiling M_E. In the sequel of the considerations made in excursus 1 we can ask: where in the window V does z_F have to lie so that from z_E arise two long tiles in a row by the basic vectors v_i, v_j, v_k, as shown in figure 26? We call such a tile also *double tile*.
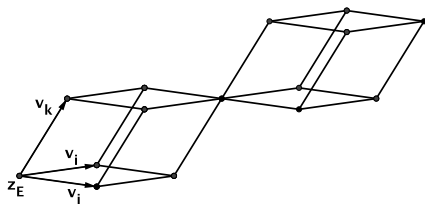

Figure 26. From z_E arises a double tile by v_i, v_j, v_k

According to the equivalences in (2.10) and (2.11) as well as the results from excursus 1 in the orthogonal space F the condition for the existence of such a

double tile spanned by v_i, v_j, v_k in the projection space E is

$$z_F \in \Omega_{(i,j,k)} \quad \text{and} \quad z_F + \underbrace{w_i + w_j + w_k}_{:=d} \in \Omega_{(i,j,k)} \tag{3.8}$$

That gives us a simple construction guide for the wanted region in V, which we denote by $\Gamma_{(i,j,k)}$:

$$\Gamma_{(i,j,k)} = \Omega_{(i,j,k)} \cap \left(\Omega_{(i,j,k)} - d \right) \tag{3.9}$$

It is $\Gamma_{(i,j,k)} \subset \Omega_{(i,j,k)}$ and also $\Gamma_{(i,j,k)}$ itself has the shape of a (somewhat smaller) long tile. Corresponding to the 20 congruent regions of type Ω there are also 20 congruent regions of type Γ.
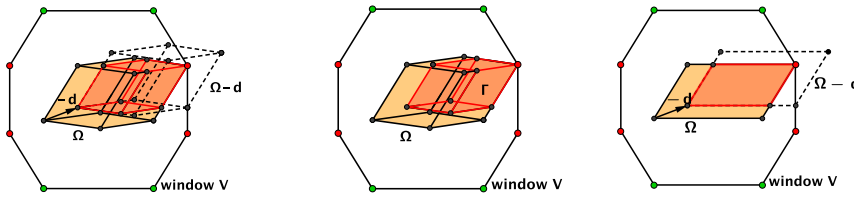

Figure 27. Construction of the region of type Γ

Summing up excursus 2 we obtain

$$z_F \in \Gamma_{(i,j,k)} \iff \text{from } z_E \text{ arises a double tile by } v_i, v_j, v_k \tag{3.10}$$

Based on this knowledge we can return to figure 25. The so far unknown red marked region corresponds to the region denoted by $\Gamma_{(-i,-j,-k)}$ and therefore (3.7) means

$$z_{F'} \in \Gamma_{(-i,-j,-k)}$$

i.e. from $z_{E'}$ arises a double tile by the basic vectors $-v_i$ and $-v_j$ as well as $-v_k$. Applying S to this results, cf. step 3, it follows that in the fine tiling SM_E from $z_{E'}$ arises a double tile by the basic vectors $\varphi^3 v_i$ and $\varphi^3 v_j$ as well as $\varphi^3 v_k$. Thus we can complete figure 22:
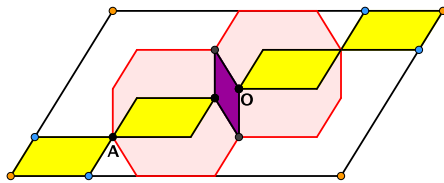

Figure 28. The two double tiles existing in the fine tiling SM_E on the two acute vertices of the coarse long tile are marked yellow.

By restricting ourselves to the left rhombic triacontahedron of figure 28 and considering theorem 3.5 we obtain the invariant structure shown in figure 29. It consists of four long tiles and four flat tiles as well as three minilenses.
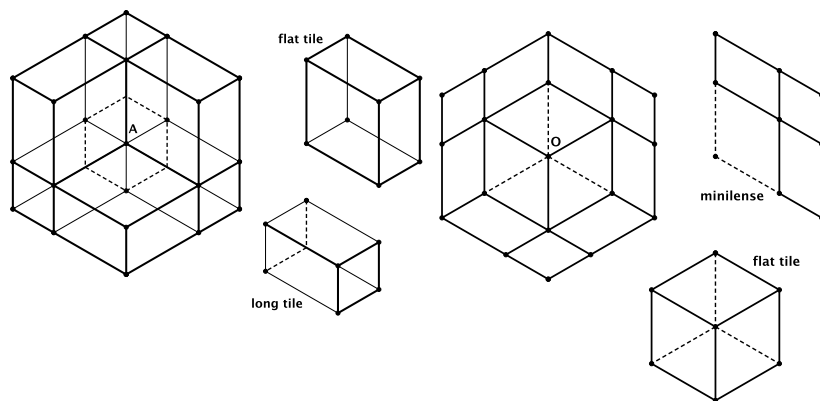
Figure 29. Structure of the left triacontahedron inside the coarse long tile

Comments on figure 29:

- In both parts of the figure (left and right), the left triacontahedron inside the long coarse tile (as shown in figure 28) is projected to the plane perpendicular to the long diagonal of the coarse tile. This projection is a regular hexagon.
  - Left: View from the acute vertex (marked with A in figure 28) of the second tile of the "doubled tile" (second long tile in Figure 28) in the direction of the long diagonal up to the obtuse vertex (marked with O in figure 28) of the connecting flat tile,
  - Right: View from O in figure 28) in the opposite direction,
- Left: At each of the three faces of the "doubled" tile (dashed lines) adjacent to A a long tile is adjoined. Any two of these long tiles having only an edge in common are connected by a flat tile, like in figure 19.
- Right: The vertex O is an obtuse vertex of the flat tile connecting the two triacontahedra. At each of the three faces of that tile (marked with dashed lines) a minilense is adjoined. Each of these three minilenses shares a face with the "doubled" tile.

The same considerations hold for the right rhombic triacontahedron of figure 28 and therefore we obtain an invariant structure inside the coarse long tile, which consists of altogether seven flat tiles and eight long tiles as well as six minilenses.
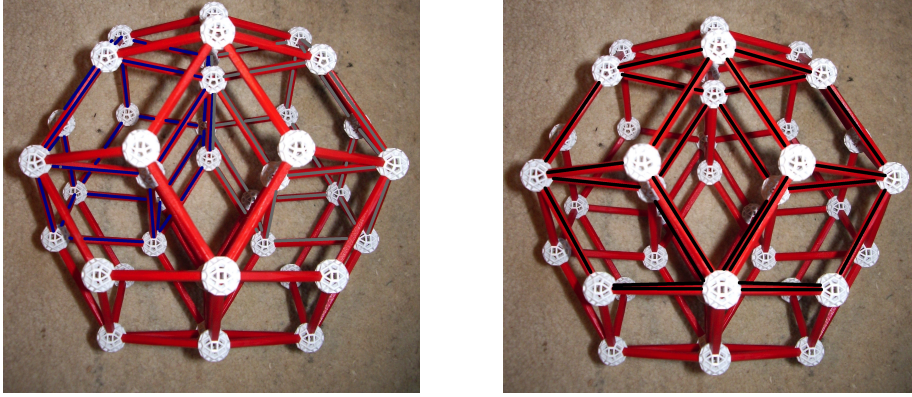
□

Figure 30. The three minilenses inside the left rhombic triacontahedron
of figure 28: marked blue and grey, left figure, and black, right figure

Hence the subdivision of the coarse long tile is known. We prove in the appendix,
see lemma 2, that each minilense can be filled with two long and two flat tiles
and the filling is unique up to isometries of the minilense. Therefore we can also
calculate the number of fine tiles "subdividing" the coarse long tile.

Theorem 3.14. *An arbitrary long tile of the coarse tiling $M_{E'}$ is filled with alto-
gether 55 long tiles and 34 flat tiles of the fine tiling SM_E, more precisely, of 550
tenths of a long tile and 340 tenths of a flat tile.*

Proof. Each of the outer lenses belonging to the ring of lenses takes part of the
coarse long tile by the ratio $\frac{3}{10}$, each of the inner lenses by the ratio $\frac{2}{10}$. This is
seen by projecting the coarse tile into the plane perpendicular to the edge carrying
the lense. The projection of a long tile into the plane perpendicular to any of its
edges is always a rhomb with angles $\frac{2}{10} \cdot 2\pi$ and $\frac{3}{10} \cdot 2\pi$, see figure 19. Thus the
coarse tile cuts out a fraction of $\frac{3}{10}$ from the lenses sitting on an outer edge and $\frac{2}{10}$
from those on the inner edges. Therefore denoting again the long tiles by L and
the flat tiles by F we obtain for the number of tiles, using theorems 3.11, 3.13 and
lemmas 2, 3:

$$\underbrace{6 \cdot (L + 4 \cdot \tfrac{1}{2} L)}_{\text{obtuse vertices}} + \underbrace{2L}_{\text{acute vertices}} + \underbrace{8L + 7F + 6 \cdot (2L + 2F)}_{\text{interior part}} +$$

$$\underbrace{6 \cdot \left(\tfrac{3}{10}(5L + 5F)\right)}_{\text{outer lenses}} + \underbrace{6 \cdot \left(\tfrac{2}{10}(5L + 5F)\right)}_{\text{inner lenses}} = 55L + 34F.$$

$\square$

4. Conclusion

In this paper, we have analyzed the icosahedral tiling: a certain class of tilings of euclidean 3-space where all edges are icosahedral vertex vectors, vectors from the center to a vertex of the regular icosahedron (also called basic vectors). We have constructed this class of tilings by projecting a subset of the regular 6-dimensional lattice $\mathbb{Z}^6 \subset \mathbb{R}^6$ onto a certain 3-dimensional affine subspace E. In fact, the symmetry group G of the icosahedron acts in a canonical way on $\mathbb{R}^6$ by integer matrices, and over the reals, this representation decomposes into two 3-dimensional irreducible subrepresentations, where the subspace E is parallel to one of these submodules. The group G acts on the unit cube $C^6 \subset \mathbb{R}^6$ with $C = (-\frac{1}{2}, \frac{1}{2})$, and this action has precisely two orbits on the set of 3-dimenisonal subcubes; their projections to E form the two tiles: a long one and a flat one. Further we have constructed an integer invertible matrix S on $\mathbb{R}^6$ commuting with the group action which is expanding on the submodule F perpendicular to E. This matrix causes what is called deflation: the subdivision of the tiling by a similar tiling whose edge length is smaller by the factor $1/\Phi^3$ where $\Phi = (1 + \sqrt{5})/2$ is the golden ratio. We observed that any vertex of the old (coarse) tiling is the common tip of 20 long tiles of the new (fine) tiling. This determines the subdivision of all coarse edges and 2-faces, using that any two vertices differing by an icosahedral vertex vector are actually joined by an edge. With some more effort, the subdivision of the tiles can also be determined, up to some small areas (lenses and minilenses) whose fillings may differ just by local isometries (however, the actual fillings of these areas are not independent from each other as explained in [6]). Thus the local structure of the tiling is everywhere the same which might be of importance for the application to quasicrystals: each atom joining the quasicrystal knows its place. As a consequence we see that the coarse long tile is filled with 55 long and 34 flat tiles of the fine tiling while for the coarse flat tile these numbers are 34 and 21; however, some of the filling tiles are decomposed into smaller fractions.

Our main references on aperiodic tilings have been [4],[13],[17]. We wish to mention in particular the work of Ogawa (see [17],[18]) who already found an invariant local structure (not complete) for this tiling, and using this he already computed the above numbers for the subdivision of the tiles. But we also like to mention the contribution of Coxeter (cf. [21]) who investigated the five isozonohedra all of which play a prominent role in our investigation. Last not least, it is hard to imagine how this paper could have been written without the help of the Zometool construction kit. Even the theoretical idea of a system of rods which is invariant under certain orthogonal projections was extremely helpful for us. Therefore we gratefully dedicate this paper to Paul Hildebrandt, founder and creative head of Zometool Inc. We encourage the reader to build the subdivisions using the Zoomtool rods since mere photographs of the three-dimensional situations are hard to understand. We also would be happy to show our own models to the interested reader.

Appendix

In this appendix we will give some details of the geometry of the icosahedron and the isozonohedra which are used in the paper.

Convexity and homothety

Lemma 1. Consider a convex set $K \subset \mathbb{R}^n$ and a homothetic map h with scale factor $0 < t < 1$ and fixed point $y \in K$. Then K is invariant under h, i.e. $h(K) \subset K$.

Proof. Without loss of generality we can choose the fixed point y as origin. Then the homothetic map h becomes $h = t \cdot I$ where I is the identity and $0 < t < 1$. Let x be a point inside K then tx is a point inside the reduced polyhedron tK. Since we have $0 < t < 1$ the point tx lies on the line segment $[0x]$ and therefore tx is inside K, because K is a convex set. Hence we obtain $h(K) \subset K$.   □

Minilense and lense

Lemma 2. For the minilense there are precisely two fillings. They are congruent and consist of two long and two flat tiles.

Proof. By fixing one of the 14 vertices of the minilense, marked orange in figure 31 (left) we consider possible tiles adjoining to this vertex inside the minilense.
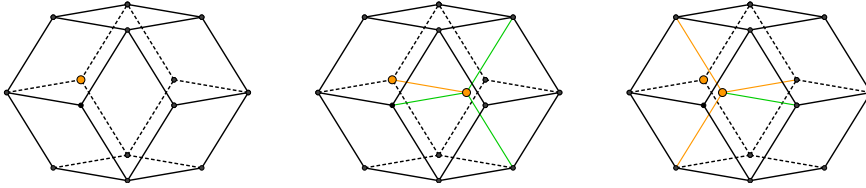

Figure 31. The filling of the minilense

Comments on figure 31:

- Possibility 1: there is an edge adjoining to the orange vertex, see middle figure. Considering theorem 3.5 the three green marked edges exist. But hence the filling of the minilense is completed: two long tiles and a flat tile adjoin to the orange vertex, a further flat tile adjoins to these three tiles inside the minilense.
- Possibility 2: there is no interior edge adjoining to the orange vertex, see right figure. Then a flat tile adjoins to the orange vertex, also marked orange. Considering theorem 3.5 the green marked edge exists and hence we obtain a further flat tile as well as to long tiles inside the minilense.

These two possibilities of filling the minilense are symmetric to the plane perpendicular to the central rhomb in figure 31.   □

Lemma 3. For the lense there are precisely ten fillings. They are pairwise congruent and consist of five long and five flat tiles.

Proof. Two of the 22 vertices of each lense are flowers, cf. figure 12 and figure 13. At one of these flowers we start filling the lense.
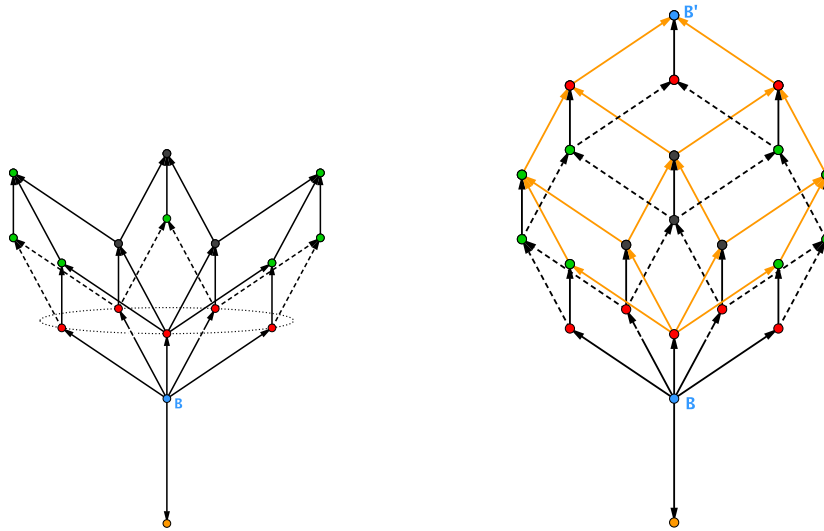

Figure 32. The filling of the lense

Comments on figure 32:

- We start at the blue marked flower vertex denoted by B. The vertex at the end of the flower stalk, an old vertex, is marked orange and the points of the blossom spanned by the petals of B are marked red and green, cf. figure 12
- Up to a fivefold rotational symmetry we can only span a long tile and two flat tiles using the petals, cf. figure 4. In the left figure the long tile is in the middle, left and right a flat tile always adjoins.
- Only the three black marked points lie inside the lense, all colored marked points are part of the shell of the lense, cf. figure 12. Hence in view of theorem 3.5 three further tiles exist: two long tiles, adjoining to the flat and the long tiles built by the petals, and a flat tile between these two long tiles. One vertex of this flat tile is the second flower vertex of the lense, denoted by B' and marked blue, see right figure.
- Therefore we obtain a structure consisting of altogether three long and three flat tiles. The rest of the interior part of the lense is a minilense, cf. figure

31. In the right figure the rhombs belonging to the lower part of shell of the minilense are marked orange.

- Note that the two flower vertices B and B' are antipodal points. Therefore the blossom spanned by the petals of B is antipodal to the blossom spanned by the petals of B'.

Because the minilense can be filled in two congruent ways, see figure 31, there are altogether ten fillings of the lense, being pairwise congruent. $\square$

Lemma 4. The ratio between the long diagonal of the long tile and the short diagonal of the flat tile corresponds to Φ^3.

Proof. The diagonals of both tiles are the projections of the diagonals of a 3-dimensional subcube C^3 of the 6-dimensional unit cube C^6 onto E. In general the
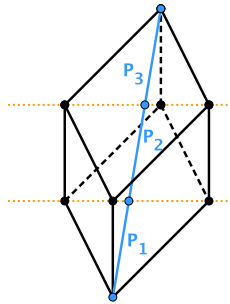

Figure 33. Diagonal of a three-dimensional cube

diagonals of any 3-cube split up into three parts, in figure 33 denoted by P_1, P_2, P_3. Since the projection preserves proportions it is sufficient to investigate

$$\frac{P_{1L}}{P_{1S}}$$

where P_{1L} denotes the P_1-part of the long diagonal of the long tile and P_{1S} the P_1-part of the short diagonal of the flat tile.

In the following we consider the long tile spanned by the pairwise direct neighbours 3,4,6 and the flat tile spanned by the pairwise indirect neighbours -1,2,5, see figure 34, left. Note that 3,4,6 and -1,2,5 lie in two parallel planes. Furthermore we assume that the two golden rectangles spanned by the vertices $\pm3, \pm5$ (marked blue) and $\pm4, \pm6$ (marked green) have edge length 2 and 2Φ. Hence we obtain

$$\frac{P_{1L}}{P_{1S}} = \frac{|OP|}{|OP'|} = \frac{|OS|}{|OS'|} = \frac{\Phi}{\Phi - 2\varphi} = \frac{\Phi}{1 - \varphi} = \frac{\Phi}{\varphi^2} = \Phi^3$$

because $|OS'| = |OS| - (|SS''| + |S''S'|)$ and $|SS''| = |S''S'| = \Phi - 1 = \varphi$, see figure 34, right.
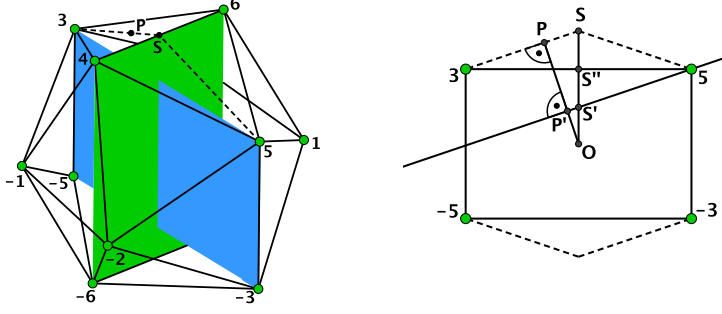
Figure 34. Icosahedron and its golden rectangles

□

Locus of deflation

Lemma 5. The region $\Omega \subset V$ to where a given vertex of any admissible long tile is projected has again the shape of a long tile. Vice versa, if $\pi_F(z) \in \Omega$ for some $z \in \mathbb{Z}^6$, then $\pi_E(z)$ is a vertex of an admissible long tile. The analogous statements hold for a flat tile.

Proof. The unit cube C^6 is the Cartesian product of two 3-dimensional subcubes: $C^6 = C_1^3 \times C_2^3 \subset \mathbb{R}_1^3 \times \mathbb{R}_2^3$ where $C_1^3 \subset \mathrm{Span}\,(e_1, e_2, e_3), C_2^3 \subset \mathrm{Span}\,(e_4, e_5, e_6)$ and $e_1, \ldots, e_6$ denote the basis vectors of the ambient space $W \cong \mathbb{R}^6$ permuted by the icosahedral group G like the oriented diagonals of the icosahedron, cf. page 4. The subcubes C_1^3 and C_2^3 are inequivalent under G, see appendix B below, and hence project to different types of tiles onto the projection space E. Further, we know by figure 1: if the E-projection π_E of a 3-dimensional subcube is a long tile, then its F-projection π_F is a flat tile, and vice versa. A subset $A \subset \mathbb{R}^6$ is called admissible if $A \subset \Sigma$ with $\Sigma = E + C^6$ or equivalently if $\pi_F(A) \subset V = \pi_F(C^6)$, see (2.9) and (2.10).

In particular, the 3-dimensional subcube $X_y := C_1^3 \times \{y\}$ with $y \in \mathbb{R}_2^3$ is admissible if and only if $y \in C_2^3$. We have $C^6 = \bigcup_{y \in C_2^3} X_y$ with $X_y = C_1^3 \times \{y\}$ and thus $\Sigma = \bigcup_{y \in C_2^3} X_y + E$. If $X_{y_o} \subset \Sigma$ for some $y_o \in \mathbb{R}_2^3$, then there is some $y \in C_2^3$ with $y - y_o \in E$. But $E \cap \mathbb{R}_2^3 = \{0\}$ and hence $y_o = y \in C_2^3$.

Choose any $x \in C_1^3$. Let $Y_x = \{x\} \times C_2^3$. Then we obtain

$$\pi_F(X_y) \subset V = \pi_F(C^6) \iff \pi_F(x, y) \in \pi_F(Y_x)$$

because $\pi_F(X_y) \subset V \iff y \in C_2^3 \iff (x, y) \in Y_x \iff \pi_F(x, y) \in \pi_F(Y_x)$.

Now a tile $T = \pi_E(X_y)$ is admissible iff $T' = \pi_F(X_y) \subset V$. If T is a long tile, then T' is flat. When T has vertex $\pi_E(x, y)$, admissability means that $\pi_F(x, y) \in T'' = \pi_F(Y_x)$, and since $T' = \pi_F(X_y)$ was flat, $\Omega = T''$ is a long tile. A similar argument holds for the flat tile. □

Coxeter's Golden Isozonohedra

According to H.M.S. Coxeter a *zonohedron* is as a convex polyhedron each of whose faces is centrally symmetrical, see [3]. If its faces are all golden rhombs then a zonohedron is called *golden isozonohedron*, cf. [3],[21]. Altogether there are five golden isozonohedra. In Coxeter's notation: the rhombic triacontahedron K_{30}, the rhombic icosahedron F_{20} and the rhombic dodecahedron B_{12}, denoted according to their discoverers *Kepler*, *Fedorov* and *Bilinski*, as well as the long and the flat tile, denoted by A_6 and O_6, where A stands for *acute* and O for *oblate*. The index specifies the number of faces, see figure 35, from left to right. They all occur in the icosahedral tilings: the two hexahedra are the two sorts of tiles, dodecahedron and icosahedron are the minilense and the lense, and the triacontahedron is the shape of the window. We want to show that these bodies are projections of the 6-dimensional cube and its subcubes onto our 3-dimensional subspace $E \subset \mathbb{R}^6$. Essentially, this has been observed already by Kowalewski [14] in 1938.
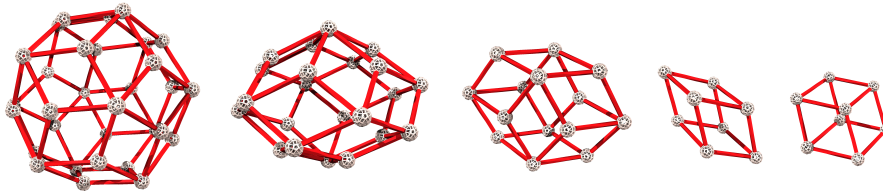

Figure 35. The five golden isozonohedra [26]

Lemma 6. $K_{30} = \pi_E(C^6)$, $F_{20} = \pi_E(C^5)$, $B_{12} = \pi_E(C^4)$, $O_6 = \pi_E(C_1^3)$ and $A_6 = \pi_E(C_2^3)$. The faces of these bodies are golden rhombs congruent to $\pi_E(C^2)$.

Proof. The icosahedral group $G \cong A_5 \times \mathbb{Z}_2$ leaves $C^6 \subset \mathbb{R}^6$ invariant. It acts transitively on the set of faces of C^6 with dimension or codimension one since it acts transitively on the oriented icosahedric diagonals corresponding to the vectors $\pm e_i$, $i = 1, \ldots, 6$, the unit normals of the codimenison-one faces. Further any two of the 6 diagonals are neighbours, hence the group G acts also transitively on the pair of diagonals, i.e. on the subsets $\{\pm e_i, \pm e_j\}$ for $i \neq j$. Each of these subsets determines a class of parallel faces of C^6 with dimension or codimension two. But G acts no longer transitively on the triples of diagonals. In fact, there are precisely two different configurations: the diagonal vectors may form a *chain*, an isosceles but not equilateral triangle, like those corresponding to e_1, e_2, e_3 or else an *equilateral triangle*, like the ones corresponding to e_4, e_5, e_6. Thus we obtain precisely two subcubes C_1^3, C_2^3 with dimension or codimension 3 which are inequivalent under G.

Since convexity is preserved under orthogonal projections, $\pi_E(C^k)$ are convex

---

[26]By courtesy of Paul Hildebrandt, Zometool Inc.

bodies, where $k = 3, 4, 5, 6$. We have already seen, cf. page 6, that $\pi_E(C^2)$ is a golden rhomb. The 2-dimensional boundary of $\pi_E(C^k)$ consists of projections of 2-dimensional cubes C^2, hence these bodies are bounded by golden rhombs. There are $\binom{k}{2}$ classes of parallel 2-dimensional faces in C^k. Every class contributes to the boundary of $\pi_E(C^k)$: if we consider a 2-face $C^2 = C^k \cap P$ for some 2-plane $P \subset \mathbb{R}^k$ and its projection $\pi_E(P) \subset E$, the hyperplane $(P + F) \cap \mathbb{R}^k$ is also projected to P. Then a parallel hypersurface $(P' + F) \cap \mathbb{R}^k$ (where P' and P are parallel) will be a support hypersurface of C^k, and the corresponding face $C^k \cap P'$ is projected to the boundary of $\pi_E(C^k)$. In fact, since C^k as well as $\pi_E(C^k)$ are invariant under the antipodal map $-I$, each 2-face appears (at least) twice, up to parallelity. But by convexity it cannot appear more than twice: the boundary of $\pi_E(C^k)$ cannot contain more than two parallel 2-faces since the plane of a 2-face in the boundary of $\pi_E(C^k)$ is a support plane, and obviously there are not more than two parallel support planes for a convex body in 3-space. Thus $\pi_E(C^k)$ has $2\binom{k}{2} = k(k-1)$ 2-faces which is the right number: 30 for $k = 6$, 20 for $k = 5$, 12 for $k = 4$ and 6 for $k = 3$. $\qquad\square$

Remark 4.1. Because of $v_1 + v_2 + v_3 + v_4 + v_5 = \sqrt{5}\,v_6$, see footnote 5, the diameter of $F_{20} = \pi_E(C^5)$ (the lens) is $\sqrt{5}\,|v|$ and the diameter of $K_{30} = \pi_E(C^6)$ (the window) is $\sqrt{5}\,|v| + |v| = 2\Phi\,|v|$ where $|v|$ is the edge length.

References

[1] Baake, M., Kramer, P., Schlottmann, M., Zeidler, D.:, *Planar patterns with fivefold symmetry as sections of periodic structures in 4-space*, Intern. J. Modern Physics B **4**, 2217 - 2268 (1990)

[2] Bohr, H.: *Zur Theorie der fastperiodischen Funktionen*, Acta math. **45** (1924), 29 - 127, **46**, 101 - 214 (1924)

[3] Coxeter, H. S. M.: *The Beauty of Geometry: Twelve Essays,* Dover Publications, Mineola 1999. Unveränderte Neuveröffentlichung von *Twelve Geometric Essays*, Southern Illinois University Press, Carbondale 1968

[4] De Bruijn, N. G.: *Algebraic Theory of Penrose's Non-Periodic Tilings of the Plane*, Indag. Math. **43**, 39 - 66 (1981)
http://www.math.brown.edu/~res/M272/pentagrid.pdf

[5] Dietl, R.: *Penrose-Muster: Unterteilung und Projektionsmethode*, Schriftliche Hausarbeit zur 1. Staatsprüfung für das Lehramt an Gymnasien, Augsburg 2008
http://myweb.rz.uni-augsburg.de/~eschenbu/ZulassungsarbeitScan.PDF

[6] Dietl, R.: *Dreidimensionale Penrose-Muster und Selbstähnlichkeit*, Dissertation, Augsburg 2011
http://myweb.rz.uni-augsburg.de/~eschenbu/diss_dietl.pdf

[7] Eschenburg, J.-H.: *Die Zahl Fünf und die Quasikristalle*, Augsburg 2004
http://myweb.rz.uni-augsburg.de/~eschenbu/penrose.pdf

[8] Eschenburg, J.-H.; Rivertz, H. J.: *Self Similar Symmetric Planar Tilings*, J. Geom. **87**, 55 - 75 (2007)

[9] Eschenburg, J.-H.; Rivertz, H. J.: *The Penrose Decagon*, Preprint (2016)

[10] Katz, A.; Duneau, M.: *Quasiperiodic Patterns and Icosahedral Symmetry*, Phys. Rev. Lett. **47**, 181 - 196 (1986)

[11] Kepler, J.: *Strena Seu de Nive Sexangula*, Frankfurt 1511. In: Gesammelte Werke, vol. IV, ed. M. Caspar and F. Hammer, München 1941, pp. 259-280, http://www.thelatinlibrary.com/kepler/strena.html

[12] Kepler, J.: *Harmoniae Mundi*, Linz 1619, https://archive.org/stream/ioanniskepplerih00kepl#page/

[13] Kramer, P.; Neri, R.: *On Periodic and Non-Periodic Space Fillings of E^m Obtained by Projection*, Acta Crystallogr. Sect. A **40**, 580 - 587 (1984)

[14] Kowalewski, G.: *Der Keplersche Körper und andere Bauspiele*, K.F. Koehlers Antiquarium, Leipzig 1938

[15] Mackay, A. L.: *De Nive Quinquangula: On the Pentagonal Snowflake*, Soviet Physics. Crystallography **26**, 517 - 522 (1981)

[16] Mackay, A. L.: *Crystallography and the Penrose Pattern*, Phys. A **114**, 609 - 613 (1982)

[17] Ogawa, T.: *On the Structure of a Quasicrystal - Three-Dimensional Penrose Transformation*, J. Phys. Soc. Japan **54**, 3205 - 3208 (1985)

[18] Ogawa, T.: *Symmetry of Three-Dimensional Quasicrystals*, Materials Science Forum **22 - 24**, 187 - 200 (1987)

[19] Penrose, R.: *Pentaplexity - a Class of Non-Periodic Tilings of the Plane*, Math. Intelligencer **2**, 32 - 37 (1979)

[20] Senechal, M.: *The Mysterious Mr. Ammann*, Math. Intelligencer **26**, 10 - 21 (2004)

[21] Senechal, M.: *Donald and the Golden Rhombohedra*. In: Davis, C.; Ellers E. W. (eds.): The Coxeter Legacy, AMS Fields, Providence 2006

[22] Shechtman D.; Blech, I.; Gratias, D.; Cahn, J. W.: *Metallic Phase with Long-Range Orientational Order and No Translational Symmetry*, Phys. Rev. Lett. **53**, 1951 - 1953 (1984)

[23] Stern, D.: *Penrose Type Tilings*, Diplomarbeit, Augsburg 2002 http://myweb.rz.uni-augsburg.de/~eschenbu/diplomarbeit.pdf

Ruth Maria Katharina Dietl
Universitätsstrasse 14
86135 Augsburg
Germany
e-mail: `rumaka@gmx.de`

Jost-Hinrich Eschenburg
Universitätsstrasse 14
86135 Augsburg
Germany
e-mail: `eschenburg@math.uni-augsburg.de`